

# Prediction of binding for a kind of non-peptic HCV NS3 serine protease inhibitors from plants by molecular docking and MM-PBSA method

Xudong Li, Wei Zhang, Xuebin Qiao and Xiaojie Xu\*

*College of Chemistry and Molecular Engineering, Peking University, Beijing 100871, China*

Received 20 August 2006; revised 27 September 2006; accepted 28 September 2006

Available online 7 October 2006

**Abstract**—In the study, molecular dynamics simulations combined with MM-PBSA (Molecular Mechanics and Poisson–Boltzmann Surface Area) technique were applied to predict the binding mode of the polyphenol inhibitor in the binding pocket of the HCV NS3 serine protease for which the ligand–protein crystal structure is not available. The most favorable geometry of three candidates from molecular docking had a binding free energy about 3 and 6 kcal/mol more favorable than the other two candidates, respectively, and was identified as the correct binding mode. In the mode, the correlation of the calculated and experimental binding affinities of all five polyphenol compounds is satisfactory indicated by  $r^2 = 0.92$ . The most favorable binding mode suggests that two galloyl residues at 3 and 4 positions of the glucopyranose ring of the inhibitors interact with SER139, GLY137, ALA157, and ASP81 by hydrogen bond interaction and with ALA156 and HIE57 by hydrophobic interaction and are essential for the activities of the studied inhibitors.

© 2006 Elsevier Ltd. All rights reserved.

## 1. Introduction

HCV NS3 protease has been used as target enzyme<sup>1–3</sup> for screening anti-HCV drugs because it is essential to the viral replication of the hepatitis C virus (HCV),<sup>4</sup> an important human pathogen causing chronic hepatitis, cirrhosis of the liver, and hepatocellular carcinoma.<sup>5</sup> Researches in recent decade years make it a well-characterized target, meanwhile its crystal structure has been solved by several groups.<sup>6–8</sup>

A number of inhibitors have been designed based on the cleavage of native substrates in recent years for the inhibition of HCV NS3 serine protease,<sup>9–15</sup> many of which are large peptidomimetic compounds with poor pharmacokinetic properties.<sup>16</sup> As one of the strategies to find new lead compounds with less peptidic character, bio-guided isolation of pharmacologically active plant components for HCV NS3 serine protease is still a valuable one.

In previous experimental work in our group, we screened the natural products in more than one hundred kinds of traditional Chinese medicine to find potential lead compounds for inhibiting HCV infection. A number of compounds with potential biological activity were identified from several plants, including *Saxifraga melanocentra*, *Rhodiola kirilowii*, *Terminalia chebula* Retz., *Terminalia chebula* Retz. Var. *tomentella* kurt, Chinese galla, and Corilagin. Some of them were characterized as polyphenol compounds, which include a glucopyranose ring with two or more galloyl residues substituting the hydrogens of hydroxyls, respectively. The compounds studied here are shown in Table 1. Considering that the crystal structure of every one of the inhibitors/HCV NS3 was not available, molecular docking studies, molecular dynamics (MD) simulations, and binding free energy calculations were performed to gain a better insight into the binding interaction between HCV NS3 serine protease and this series of inhibitors.

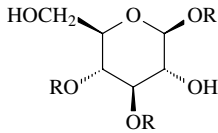
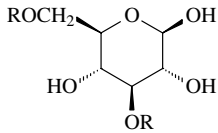
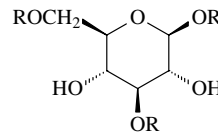
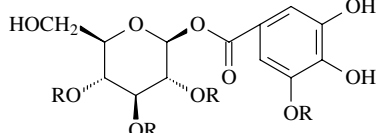
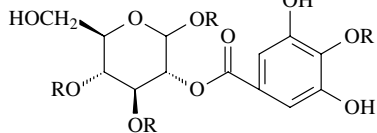
## 2. Results and discussion

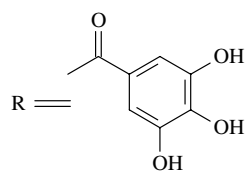
All 30 decoys from docking are grouped into three clusters by the hierarchical clustering using relative rms. In

**Keywords:** MM-PBSA; Molecular dynamics; Docking; Polyphenol; Inhibitor; HCV NS3 protease.

\* Corresponding author. Tel.: +86 1062757456; fax: +86 1062751708; e-mail: [xiaojxu@pku.edu.cn](mailto:xiaojxu@pku.edu.cn)

**Table 1.** Structures, activities, and resource of polyphenol compounds with potential biological activity for inhibiting HCV infection identified from several plants

Compound	Structure and name	Molecular weight	IC <sub>50</sub> (μg/mL) (μM)	Plant resource
1	 1,3,4-tri-O-galloyl-β-D-glucose	C <sub>27</sub> H <sub>24</sub> O <sub>18</sub> , 636	0.64(1.0)	Saxifraga melanocentra
2	 3,6-di-O-galloyl-β-D-glucose	C <sub>20</sub> H <sub>20</sub> O <sub>14</sub> , 484	460(949.7)	Saxifraga melanocentra
3	 1,3,6-tri-O-galloyl-β-D-glucose	C <sub>27</sub> H <sub>24</sub> O <sub>18</sub> , 636	6.42(10.09)	Terminalia chebula Retz.
4	 1-O-(3-O-Galloyl-galloyl)-2,3,4-tri-O-galloyl-β-D-glucose	C <sub>41</sub> H <sub>32</sub> O <sub>26</sub> , 940	0.64(0.68)	Saxifraga melanocentra
5	 2-O-(4-O-Galloyl-galloyl)-1,3,4-tri-O-galloyl-β-D-glucose	C <sub>41</sub> H <sub>32</sub> O <sub>26</sub> , 940	0.62(0.66)	Rhodiola kirilowii



every cluster, the proposed interaction mode of the ligand with the HCV NS3 serine protease active site is determined as the highest scored conformation among all conformation as according to the pmf-score. MD simulations of 100 ps were performed for all three binding modes of HCV NS3 serine protease/compound **5** complexes. For the binding mode I of compound **5**, root-mean-square deviation (RMSD) from the starting structure from docking for the main chain atoms of protein and all atoms of ligand are shown as a function of time for the 100 ps runs in Figure 1. After 50 ps simulation, RMSD of the main chain is smaller than 0.10 Å and that of the ligand is smaller than 0.50 Å, which indi-

cates that the system was equilibrated and the trajectories after 50 ps can be applied to collect snapshots for further analyses.

Table 2 lists the calculated relative binding free energies of three candidates, as well as the components of molecular mechanics and solvation energies. The binding free energy of binding mode I is −17.47 kcal/mol, about 3 kcal/mol more negative than the second best binding mode (binding mode III, −14.28 kcal/mol) and is most favorable among the three binding modes. Moreover, the binding mode I has the lowest van der Waals energy, gas-phase electrostatic energy, and nonpolar solvation

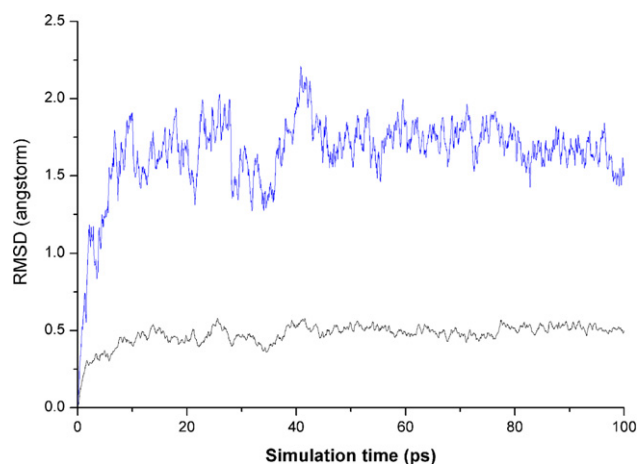


**Figure 1.** Root-mean-square deviations (Å) of all main chain atoms of HCV NS3 serine protein (black line) and all atoms of compound **5** (blue line) during 100 ps MD simulations compared with the first coordinate frame.

energy, but the gas-phase electrostatic contributions to the energy are canceled against the contribution to the energy from polar solvation. The hydrophobic interaction energy ( $\Delta G_{SA} + \Delta E_{vdw} = -48.63$  kcal/mol) is comparable with the electrostatic energy ( $\Delta G_{PB} + \Delta E_{ele} = 31.10$  kcal/mol) for formation of complex between protein and compound **5**, which shows that no predominant factor leads to stable complex formation.

Figure 2 shows the positions and orientations of compound **5** after 100 ps simulation for three possible binding modes. There are significant differences among these orientations and positions of three candidates. In binding mode III, compared to in binding mode I, compound **5** adopts a reverse turn conformation around an axis that passes nearly parallelly through two galloyl residues at 1 and 4 positions of inhibitors. The galloyl residue at 4 position cannot be embed deeply into active site like the one in binding mode I due to its upper substitution position at the glucopyranose ring of inhibitors and only forms two hydrogen bonds with GLY137 and LEU135, respectively. The galloyl residue at 3 position interacts with LYS136 by a hydrogen bond and hydrophobic interaction because of its orientation. The conformation of compound **5** in binding mode II has a similar position as binding mode III, but the galloyl residue at 4 position directs to ASP81 and is not located in the binding cleft. Although it forms a hydrogen bond with ASP81 and the hydrophobic interactions with ALA156 and HIE57 which occur in binding mode I, the salt bridge with SER139 and the hydrogen bond with GLY137 are not maintained. In addition, in both

conformations of the binding mode II and III, inhibitors form other hydrogen bonds with CYS159 and other hydrophobic interaction with VAL158. Above analysis about interactions between inhibitor and protein shows that in both error modes not only the number of formed interactions is fewer than in bonding mode I, but also the interactions important to activity in previous publications<sup>17</sup> are more or less absent. These may explain why the most favorable geometry of three candidates has a binding energy about 3 and 6 kcal/mol more favorable than the other two candidates, respectively.

To better understand the interaction between protein and compound **5** in binding mode I, we analyzed hydrogen bond and hydrophobic interactions using LIGPLOT program<sup>18</sup> (Fig. 3). One salt bridge forms between two hydroxy oxygen atoms of the galloyl residue at 4 position of the glucopyranose ring of compound **5** and SER139 and one hydrogen bond forms between one of the hydroxy oxygen atoms of the galloyl residue and GLY137, while the other hydrogen bond occurs between the carbonyl oxygen atom of the galloyl and ALA157. Like in most non-covalent inhibitors of HCV NS3, these interactions would provide a significant contribution to binding. This can be further validated by the fact that compounds **2** and **3** without the 4-position-galloyl residue, as well as the predicted binding mode II of compound **5**, in which the galloyl residue is not oriented to SER139 of the catalytic triad correctly, yield lower experimental and calculated binding free energies. Another prominent residue for the binding of inhibitor is the galloyl residue at 3 position of the glucopyranose ring of compound **5**. In the structure of complex, the galloyl interacts with ASP81 through a salt bridge, with HIE57 and ALA156 through hydrophobic interactions. Moreover,  $\pi$ - $\pi$  stacking interaction between the indole ring of HIE57 and benzene ring of the galloyl also stabilizes the binding of ligand and protein. This can be used to explain why the binding affinity of the predicted binding mode III is more positive than the binding mode I. The above results suggest that two galloyl residues at 3 and 4 positions of inhibitors are essential for activity. In addition, inhibitor forms other hydrogen bonds with ARG123 and CYS159 and other hydrophobic interaction with VAL158.

Because the galloyl group at 4 position is located deeply in the binding pocket and produces close contact with the receptor, introduction of large groups on the galloyl will be unfavorable to the surface and energetic complementarity between ligand and receptor. The surface of protein contacting with the galloyl at 3 position is a hydrophobic area which is formed by several residues: ALA156, HIE57, and ARG155. This means that substi-

**Table 2.** Comparison among calculated relative binding free energies and their components of three binding candidates

Binding mode	$\Delta E_{ele}$	$\Delta E_{vdw}$	$\Delta E_{inter}$	$\Delta \Delta G_{PB}$	$\Delta \Delta G_{SA}$	$\Delta G_{calc}$
I	-80.55	-42.08	-122.57	111.65	-6.55	-17.47
II	-46.94	-37.23	-84.18	75.07	-5.17	-14.28
III	-50.98	-36.44	-87.28	81.84	-5.93	-11.38

All energies are in kcal/mol.

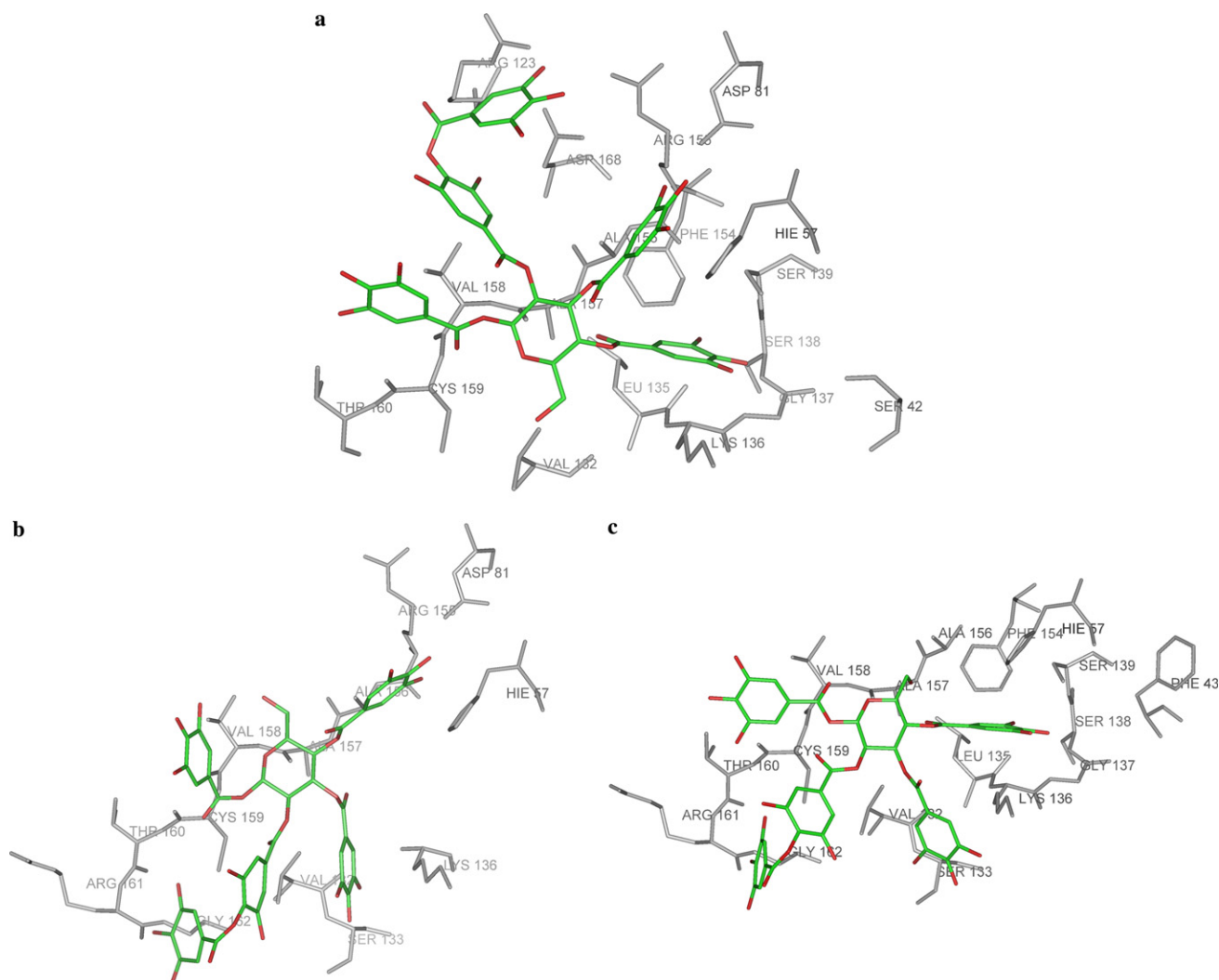


**Figure 2.** Orientations and positions of compound **5** in three binding modes after 100 ps MD simulation (a) binding mode I, (b) binding mode II, and (c) binding mode III.

tution of the carbonyl group or the phenolic hydroxyl group, which is not involved in formation of a salt bridge with ASP81, with the other nonpolar groups should improve the binding affinities of ligand. Moreover, if we change the hydroxyl group at 6 position of a ligand to a large hydrophobic group and make the ligand interact with LYS136 and VAL132 through hydrophobic interactions, the biological activities of the ligand should be probably improved.

The complex structures of HCV NS3 serine protease with other four analogues (compounds **1–4**) were constructed using the binding modes I of HCV NS3/compound **5** as the template in Sybyl modeling program. The binding free energy of each complex was obtained after MD simulation and MM-PBSA method with the same parameters as the binding modes I of HCV NS3/compound **5**, respectively. All results are list in Table 3. In the binding mode, the rank order of predicted binding free energies of five compounds is in good agreement with the experimental results (Fig. 4). The correlation coefficient between the predicted and exper-

imental binding energies is 0.96. This further verifies the predicted binding mode of this series of complex rational.

### 3. Conclusion

In this study, we predict a binding mode in which a series of polyphenol compounds, which include a glucopyranose ring with two or more galloyl residues substituting the hydrogens of hydroxyls respectively, interact with HCV NS3 serine protease by FlexX, explicit solvent MD simulations, and MM-PBSA method. In the binding mode, the correlation coefficient between the predicted relative free binding energies and experimental values of five compounds is 0.96. Two galloyl residues at 3 and 4 positions of glucopyranose ring of inhibitors are predicted to interact with SER139, GLY137, ALA157, and ASP81 by hydrogen bond interaction and with ALA156 and HIE57 by hydrophobic interaction and to be essential for the activities of the series of inhibitors. Therefore, correct

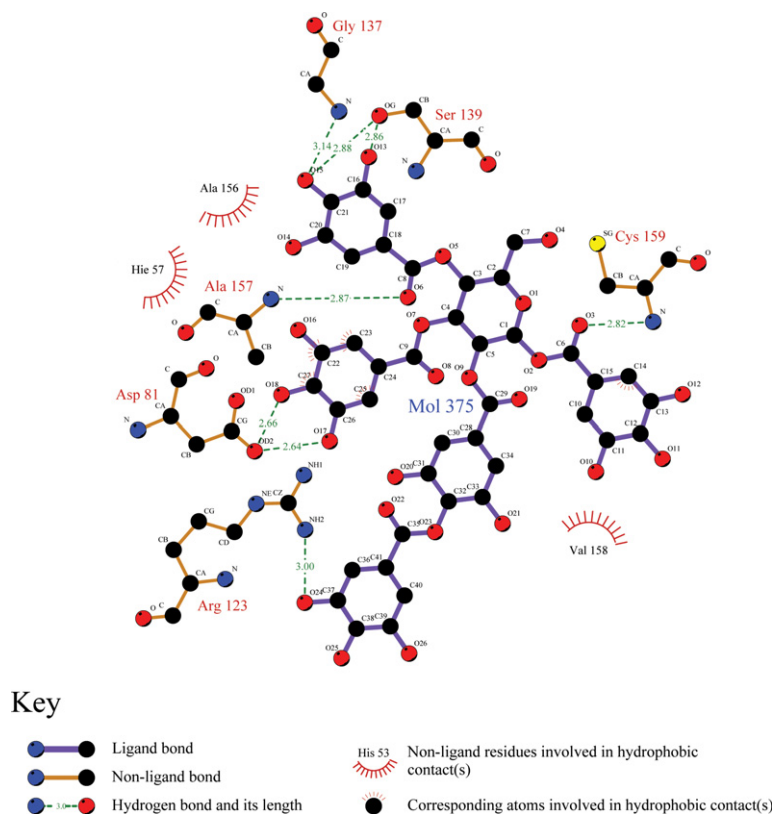


**Figure 3.** Schematic diagrams showing hydrogen bond interactions and hydrophobic interactions between HCV NS3 serine protease and compound 5 in mode I.

**Table 3.** Calculated binding free energies and experimental results of five complexes (kcal/mol)

No.	$\Delta E_{\text{ele}}$	$\Delta E_{\text{vdw}}$	$\Delta E_{\text{inter}}$	$\Delta \Delta G_{\text{PB}}$	$\Delta \Delta G_{\text{SA}}$	$\Delta G_{\text{calc}}$	$\Delta G_{\text{expt}}^a$
1	−71.55	−30.03	−101.50	89.52	−5.24	−17.22	−8.181
2	−56.47	−21.22	−77.68	67.11	−4.27	−14.83	−4.119
3	−59.70	−26.04	−85.73	73.78	−4.51	−16.46	−6.812
4	−79.13	−39.25	−118.33	106.67	−6.59	−18.25	−8.409
5	−80.55	−42.08	−122.57	111.65	−6.55	−17.47	−8.427

All energies are in kcal/mol.

<sup>a</sup> Experimental binding free energies are calculated from  $\text{IC}_{50}$  using the following formula:  $\Delta G_{\text{expt}} \approx RT \ln \text{IC}_{50}$ , where  $R$  is ideal gas constant,  $T$  is temperature in K (298 K is used in this paper).

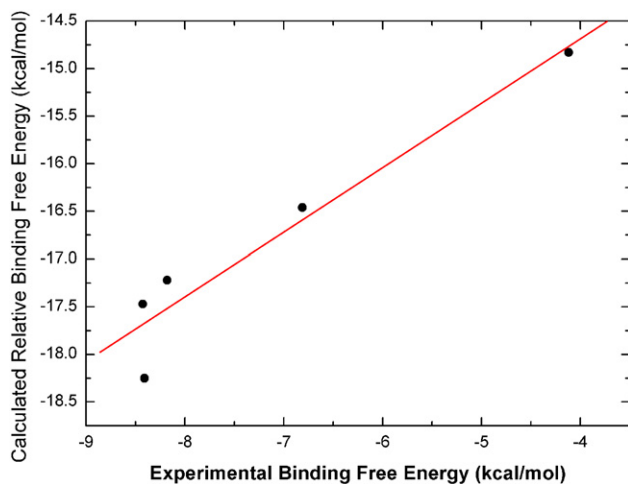


**Figure 4.** Calculated relative binding free energies ( $\Delta G_{\text{calc}}$ ) versus experimentally determined binding free energies ( $\Delta G_{\text{exp}}$ ) for the series of inhibitors.

binding mode of 2-*O*-(4-*O*-galloyl)galloyl-1,3,4-tri-*O*-galloyl- $\beta$ -D-glucose can be used as a novel scaffold for anti-HCV for the further reconstruction and design of new protease inhibitors.

## 4. Methods

### 4.1. Screening of inhibitors

We adopt the method reported by Nobuko Kakiuchi et al.<sup>19</sup> to express and purify the HCV NS3 serine protease. The functional monomer MAA (4.7 mmol), the cross-linker Trim (24 mmol), and the initiator AIBN (32 mg) were used to prepare the polymeric carrier in a test tube. The frontal affinity chromatographic experiments were done at room temperature as previously described.<sup>20</sup> HCV NS3 serine protease was immobilized on the polymeric material and then packed wetly in the



affinity columns (PEEK tubing,  $0.75 \times 50$  mm). The sample solution (in 2 mM, pH 6.7, NH<sub>4</sub>Ac) and methanol were mixed in the *T* valve and then entered the detector of Mariner electrospray ionization time-of-flight (ESI-TOF) mass spectrometer (PE Biosystems, USA ESI-TOF MS. A). Screening the crude extracts from *Saxifraga melanocentra*, *Rhodiola kirilowii*, and *Terminalia chebula* Retz. by HCV NS3 serine protease column, five polyphenol compounds **1**, **2**, **3**, **4**, and **5**, which inhibited HCV NS3 serine protease with IC<sub>50</sub> of 1.00, 949.70, 10.09, 0.68, and 0.80  $\mu$ M, were obtained, respectively.

#### 4.2. Molecular docking

All compound structures were constructed and minimized using the SYBYL modeling program. We used the crystal structure of HCV NS3/NS4/peptide Inhibitor (1dy8)<sup>7</sup> as the template to generate the receptor active site. The FlexX module<sup>21</sup> in SYBYL 7.0 was used to dock all compounds into the active site of the crystallographic HCV NS3/NS4 structure, which was defined as all residues within 6.5 Å away from the peptide inhibitor in original complex. Using an incremental construction algorithm, FlexX is a fast method to dock small conformationally flexible ligands into fixed protein binding sites. For every compound, 30 conformations were obtained from docking and were scored by Cscore program. Three binding modes were identified after cluster analysis on all decoys. The best conformation in every cluster was selected for subsequent MD simulations by consensus score and pmf-score<sup>22</sup> based on our previous work about the comparison of several empirical scoring functions.<sup>23</sup>

#### 4.3. Molecular dynamics (MD) simulations

Several sets of MD simulations were performed with Amber 8.0 package using a time step of 0.5 fs and the Amber force field.<sup>24</sup> All of complexes were solvated using a shell of TIP3PBOX water molecules<sup>25</sup> with a closeness parameter of 16 Å away from the boundary of any protein and ligand atoms. Counterions (Cl<sup>−</sup>) were added to neutralize the charge of system. Each solvated system was first energy minimized for 1000 steps using the steepest descent method followed by conjugate gradient to remove bumps possibly existing between solvent molecules and the proteins. Conjugate gradient energy minimizations were performed repeatedly four times using the positional restraints to all heavy atoms with 1000, 500, 100, and 0 kcal/mol/Å force constants in sequence. The maximum number of cycles of minimization was 20,000 and the convergence criterion for the energy gradient was 0.5 cal/mol/Å. Further 100 ps MD simulation was carried out. In the simulations all atoms of water molecules beyond 8 Å from the atoms of the complexes were held fixed. All simulations were performed using the SANDER module of AMBER8.

#### 4.4. MM-PBSA

Using the MM/PBSA method,<sup>26–28</sup> the binding free energies between receptor and inhibitors were calculated

for snapshot structures taken from the MD trajectory of the system. From the latter 50-ps complex-ligand MD trajectories of HCV NS3 and polyphenol inhibitors, 50 snapshots were taken at even intervals for the binding energy analyses in the study. In the MM/PBSA method the binding free energy ( $\Delta G_{\text{bind}}$ ) was estimated by summing the molecular mechanical gas-phase energies ( $\Delta E_{\text{MM}}$ ), solvation free energies ( $\Delta G_{\text{solv}}$ ), and entropy contributions ( $T\Delta S$ ) of the binding process:

$$\begin{aligned}\Delta G_{\text{binding}} &= \Delta G_{\text{gas}} - \Delta G_{\text{solv}}^{\text{Receptor}} - \Delta G_{\text{solv}}^{\text{Ligand}} + \Delta G_{\text{solv}}^{\text{Complex}} \\ &= \Delta H_{\text{gas}} - T\Delta S - \Delta G_{\text{PBSA}}^{\text{Receptor}} - \Delta G_{\text{PBSA}}^{\text{Ligand}} + \Delta G_{\text{PBSA}}^{\text{Complex}} \\ &= \Delta H_{\text{gas}} - T\Delta S - \Delta G_{\text{PBSA}}^{\text{Receptor}} - \Delta G_{\text{PBSA}}^{\text{Ligand}} + \Delta G_{\text{PBSA}}^{\text{Complex}}\end{aligned}$$

$$\begin{aligned}\Delta H_{\text{gas}} &\approx \Delta E_{\text{gas}} = \Delta E_{\text{intra}} + \Delta E_{\text{elec}} + \Delta E_{\text{vdw}} \\ \Delta \Delta G_{\text{PB}} &= \Delta G_{\text{PB}}^{\text{Complex}} - \left( \Delta G_{\text{PB}}^{\text{Receptor}} + \Delta G_{\text{PB}}^{\text{Ligand}} \right) \\ \Delta \Delta G_{\text{SA}} &= \Delta G_{\text{SA}}^{\text{Complex}} - \left( \Delta G_{\text{SA}}^{\text{Receptor}} + \Delta G_{\text{SA}}^{\text{Ligand}} \right)\end{aligned}$$

where  $\Delta E_{\text{gas}}$  is the average molecular mechanics energy term that is approximated as the sum of internal strain energy ( $\Delta E_{\text{intra}}$ ), van der Waals energy ( $\Delta E_{\text{vdw}}$ ), and electrostatic energy ( $\Delta E_{\text{elec}}$ ).  $\Delta E_{\text{intra}}$  is the average internal strain energies in bonds, angles, and torsion angles. The solvation free energy,  $\Delta G_{\text{solv}}$ , can be further divided into contributions from polar solvation ( $\Delta G_{\text{PB}}$ ) and nonpolar solvation term ( $\Delta G_{\text{SA}}$ ) using a continuum representation of the solvent. The polar contribution ( $\Delta G_{\text{PB}}$ ) to the solvation energy was calculated using the DELPHI program with PARSE atom radii and standard Parm94 charges for amino acids. A grid resolution of 0.5 Å/grid point was used in the Delphi calculations. The dielectric constant was set to 1 for interior solute and 80 for exterior water. The nonpolar contributions ( $\Delta G_{\text{SA}}$ ) are estimated using a simple equation:

$$\Delta G_{\text{SA}} = \gamma \times \text{SASA} + b \text{ kcal mol}^{-1}$$

SASA is the solvent-accessible surface area that was estimated using the MSMS algorithm with probe radius of 1.4 Å. The surface tension proportionality constant  $\gamma$  and the free energy of nonpolar solvation for a point solute  $b$  were set to 0.00542 kcal/mol/Å<sup>2</sup> and 0.092 kcal/mol, respectively. The entropy contributions in the binding free energies for this series of inhibitors should have no remarkable differences because of their similarities of their structures. Moreover, the prediction of entropy contribution computed by the normal-mode analysis using the nmode module in AMBER 8 has relatively large error.<sup>29</sup> So, entropy contributions ( $T\Delta S$ ) in the binding free energies were not estimated in this study.

#### Acknowledgments

The project is supported by NSFC (National Nature Science Foundation of China) 20375002.

## References and notes

1. Tan, S.; He, Y.; Huang, Y.; Gale, M., Jr. *Curr. Opin. Pharmacol.* **2004**, *4*, 465.
2. Kakiuchi, N.; Hijikata, M.; Komoda, Y.; Tanji, Y.; Hirowatari, Y.; Shimotohno, K. *Biochem. Biophys. Res. Commun.* **1995**, *210*, 1059.
3. Sudo, K.; Matsumoto, Y.; Matsushima, M.; Fujiwara, M.; Konno, K.; Shimotohno, K.; Shigeta, S.; Yokata, T. *Biochem. Biophys. Res. Commun.* **1997**, *238*, 643.
4. Kolykhalov, A. A.; Mihalik, K.; Feinstone, S. M.; Rice, C. M. *J. Virol.* **2000**, *74*, 2046.
5. Tan, S.; Pause, A.; Shi, Y.; Sonenberg, N. *Nat. Rev. Drug Disc.* **2002**, *1*, 867.
6. Yao, N. H.; Reichert, P.; Taremi, S. S.; Prorise, W. W.; Weber, P. C. *Structure* **1999**, *7*, 1353.
7. Di Marco, S.; Rizzi, M.; Volpari, C.; Walsh, M. A.; Narjes, F.; Colarusso, S.; De Francesco, R.; Matassa, V. G.; Sollazzo, M. *J. Biol. Chem.* **2000**, *275*, 7152.
8. Archer, S. J.; Camac, D. M.; Wu, Z. J.; Farrow, N. A.; Domaille, P. J.; Wasserman, Z. R.; Bukhtiyarova, M.; Rizzo, C.; Jagannathan, S.; Mersinger, L. J.; Kettner, C. A. *Chem. Biol.* **2002**, *9*, 79.
9. De Francesco, R.; Migliaccio, G. *Nature* **2005**, *436*, 953.
10. Malancona, S.; Colarusso, S.; Ontoria, J. M.; Marchetti, A.; Poma, M.; Stansfield, I.; Laufer, R.; Di Marco, A.; Taliani, M.; Verdirame, M.; Gonzalez-paz, O.; Matassa, V. G.; Narjes, F. *Bioorg. Med. Chem. Lett.* **2004**, *14*, 4575.
11. Llinas-Brunet, M.; Bailey, M. D.; Ghiro, E.; Gorys, V.; Halmos, T.; Poirier, M.; Rancourt, J.; Goudreau, N. *J. Med. Chem.* **2004**, *47*, 6584.
12. Andrews, D. M.; Barnes, M. C.; Dowle, M. D.; Hind, S. L.; Johnson, M. R.; Jones, P. S.; Mills, G.; Patikis, A.; Pateman, T. J.; Redfern, T. J.; Ed Robinson, J.; Slater, M. J.; Trivedi, N. *Org. Lett.* **2003**, *5*, 4631.
13. Zhang, R.; Durkin, J. P.; Windsor, W. T. *Bioorg. Med. Chem. Lett.* **2002**, *12*, 1005.
14. Ingallinella, P.; Fattori, D.; Altamura, S.; Steinkuhler, C.; Koch, U.; Cicero, D.; Bazzo, R.; Cortese, R.; Bianchi, E.; Pessi, A. *Biochemistry* **2002**, *41*, 5483.
15. Beevers, R.; Carr, M. G.; Jones, P. S.; Jordan, S.; Kay, P. B.; Lazell, R. C.; Raynham, T. M. *Bioorg. Med. Chem. Lett.* **2002**, *12*, 641.
16. West, M. L.; Fairlie, D. P. *Trends Pharmacol. Sci.* **1995**, *16*, 67.
17. Fischmann, T. O.; Weber, P. C. *Curr. Pharm. Des.* **2002**, *8*, 2533.
18. Wallace, A. C.; Laskowski, R. A.; Thornton, J. M. *Protein Eng.* **1995**, *8*, 127.
19. Kakiuchi, N.; Hijikata, M.; Komoda, Y.; Tanji, Y.; Hirowatari, Y.; Shimotohno, K. *Biochem. Biophys. Res. Commun.* **1995**, *210*, 1059.
20. Schriemer, D. C.; Bundle, D. R.; Li, L.; Hindsgaul, O. *Angew. Chem., Int. Ed.* **1998**, *37*, 3383.
21. Kramer, B.; Rarey, M.; Lengauer, T. *Proteins* **1999**, *37*, 228.
22. Muegge, I.; Martin, Y. C. *J. Med. Chem.* **1999**, *42*, 791.
23. Li, X.; Hou, T.; Xu, X. *Acta Phys.-Chim. Sin.* **2005**, *21*, 504.
24. Wang, J.; Wolf, R. M.; Caldwell, J. W.; Kollman, P. A.; Case, D. A. *J. Comput. Chem.* **2004**, *25*, 1157.
25. Jorgensen, W. L.; Chandrasekhar, J.; Madura, J. D.; Impey, R. W.; Klein, M. L. *J. Chem. Phys.* **1983**, *79*, 926.
26. Wang, J.; Morin, P.; Wang, W.; Kollman, P. A. *J. Am. Chem. Soc.* **2001**, *123*, 5221.
27. Hou, T. J.; Zhu, L. L.; Chen, L. R.; Xu, X. J. *J. Chem. Inf. Comput. Sci.* **2003**, *43*, 273.
28. Kollman, P. A.; Massova, I.; Reyes, C.; Kuhn, B.; Huo, S.; Chong, L.; Lee, M.; Lee, T.; Duan, Y.; Wang, W.; Donini, O.; Cieplak, P.; Srinivasan, J.; Case, D. A.; Cheatham, T. E., III *Acc. Chem. Res.* **2000**, *33*, 889.
29. Hou, T. J.; Guo, S. L.; Xu, X. J. *J. Phys. Chem. B* **2002**, *106*, 5527.